ELECTROCHEMISTRY

Environmentally-friendly aqueous Li (or Na)-ion battery with fast electrode kinetics and super-long life

Xiaoli Dong, Long Chen, Jingyuan Liu, Servane Haller, Yonggang Wang,* Yongyao Xia*

Current rechargeable batteries generally display limited cycle life and slow electrode kinetics and contain environmentally unfriendly components. Furthermore, their operation depends on the redox reactions of metal elements. We present an original battery system that depends on the redox of I^-/I_3^- couple in liquid cathode and the reversible enolization in polyimide anode, accompanied by Li^+ (or Na^+) diffusion between cathode and anode through a Li^+/Na^+ exchange polymer membrane. There are no metal element–based redox reactions in this battery, and Li^+ (or Na^+) is only used for charge transfer. Moreover, the components (electrolyte/electrode) of this system are environment-friendly. Both electrodes are demonstrated to have very fast kinetics, which gives the battery a supercapacitor-like high power. It can even be cycled 50,000 times when operated within the electrochemical window of 0 to 1.6 V. Such a system might shed light on the design of high-safety and low-cost batteries for grid-scale energy storage.

INTRODUCTION

Because of the limited oil storage and the global warming threats, building a low-carbon society supported by sustainable energy, such as wind and solar energy, has been a worldwide topic. Efficient utilization of intermittent renewable energy sources, such as wind or solar energy, needs flexible storage systems (1–7), but the options are presently dominated by pumped hydroelectric storage that is limited to a specific geographic location (1, 2). Battery systems should be a viable solution, provided that lower costs can be obtained (2). A long life (>10,000 cycles) is key to keeping costs down (1), but the life of conventional batteries is far from this value. Furthermore, the operation of current batteries depends on the redox reaction of metal elements (8, 9). The fabrication of electrodes from limited ores increases battery costs (8). In addition, safety requests of batteries for grid-level energy storage are much higher compared with current portable batteries. All current batteries contain toxic and/or environmentally unfriendly components, such as toxic nonaqueous electrolyte in current Li-ion batteries, acid/alkaline electrolyte in Ni-MH or lead-acid batteries, and toxic electrode materials (for example, Pb in lead-acid batteries, Cd in Ni-Cd batteries, VO_x in vanadium flow batteries, and Br_2 in Zn-Br$_2$ flow batteries).

In recent years, many efforts have been made to develop low-cost and highly safe batteries for grid-scale energy storage (2). Classical Li-ion batteries have high energy densities but are too expensive, and their cycle life and safety are not suitable for grid applications (2). Although Na-S batteries are currently the most credible option, on-field accidents have proven the lack of safety of this technology (2). Redox flow batteries, including traditional aqueous Zn-Br$_2$ flow batteries, have restricted energy densities because of the limited achievable maximum concentrations of the soluble redox species (3). Nonaqueous Li-S and Li-iodine redox flow batteries have been recently developed to reach higher energy densities. However, both of these batteries face numerous challenges such as high cost, difficulty to scale-up, flammable components, the low conductivity of the nonaqueous electrolyte, and so on

(10–13). New concepts are emerging on how to overcome these issues. For example, the recently reported "metal-free organic-inorganic aqueous flow battery" totally avoids the use of metal element–based electrodes (7), and thus reduces the cost from the electrode material. However, its limited cycle life (about 15 cycles) should be further improved for future stationary energy storage (1). Whereas a high-energy density aqueous zinc-polyiodide flow battery using a highly soluble iodide/triiodide redox couple has been reported, the cycling behavior presented is only 40 cycles (3). Wang et al. (6) have recently developed an all-liquid Li-Sb battery for grid-level energy storage, which greatly reduces the costs from both electrode materials and battery fabrication. However, the high operation temperature (450°C) and molten metallic electrodes (Li and Sb) may be a safety concern. On the other hand, aqueous Li (or Na)-ion batteries, which are based on the Li^+/Na^+ intercalation electrode in aqueous electrolyte, are attracting considerable attention for electrochemical energy storage because of their high safety, low cost for battery fabrication, and high rate. However, the progress of aqueous Li (or Na) batteries is held back by the limited cycle life. To date, the longest life achieved for aqueous Li (or Na)-ion batteries is only about 1000 cycles (14–22). Although Li ion (or Na ion) has an inherently small diameter, its repeated intercalation/de-intercalation over thousands of cycles gradually destroys the crystalline framework of electrode materials (that is, intercalation compound), finally resulting in capacity fading. Recently, an alternative approach that uses an electroactive organic material with a conjugated carbonyl group as the anode material for aqueous batteries has been proposed (23). However, the organic anode is still coupled with an intercalation compound cathode to form a full cell, which displays a limited cycle life (less than 200 cycles) (23).

Here, we present an original battery system that depends on the reversible redox reaction of I^-/I_3^- couple in liquid cathode and on the reversible enolization of $(C=O)_n/(C-O-Li/Na)_n$ in anode, accompanied by Li (or Na)-ion transfer between cathode and anode through a Li^+/Na^+ exchange polymer membrane. The electrode reactions are independent of metal element–based redox reactions in conventional batteries. We also demonstrate that the kinetics of both electrodes are not limited by the ion diffusion process or phase conversion, and thus, this architecture has the promise of achieving battery-level energy density combined

Department of Chemistry and Shanghai Key Laboratory of Molecular Catalysis and Innovative Materials, Institute of New Energy, iChEM (Collaborative Innovation Center of Chemistry for Energy Materials), Fudan University, Shanghai 200433, China. *Corresponding author. E-mail: ygwang@fudan.edu.cn (Y.W.); yyxia@fudan.edu.cn (Y.X.)

with the cycle life and power density of supercapacitors. Both electrodes and electrolyte are environment-friendly.

RESULTS

Operation mechanism of a full cell

As shown in Fig. 1A, the battery includes a liquid cathode that is based on water-soluble redox couples of I^-/I_3^- and aqueous electrolyte containing Li^+ (or Na^+), a solid-state polyimide anode, or a polymer Li^+/Na^+ exchange membrane (Nafion 117 treated with $LiNO_3$ or $NaNO_3$) to separate cathode and anode. Its operation mechanism is similar to a conventional Li-ion battery: I^- ions are oxidized into I_3^- ions on charge, and simultaneously, Li ions (or Na ions) in liquid cathode diffuse across the ion exchange separator to react with polyimide anode to form Li_x-polyimide or (Na_x-polyimide) through an "enolization process" $[(C=O)_n \rightarrow (C-O-Li/Na)_n]$. Discharge reverses the charge process. The electrons, of course, pass around the external circuit. The electrode reactions over charge/discharge are given in Fig. 1B.

Electrochemical behavior of single electrodes

The polyimide was prepared from 1,4,5,8-naphthalenetetracarboxylic dianhydride (NTCDA) according to a previous report (24), and thus was named NTCDA-derived polyimide (that is, PNTCDA). The purity of the as-prepared PNTCDA was confirmed by Fourier transform infrared (FT-IR) (fig. S1). Before the fabrication of a full cell, the electrochemical performance of PNTCDA in aqueous electrolyte was

investigated by cyclic voltammetry (CV) and galvanostatic charge/discharge measurements with a three-electrode system. Figure 2A shows the CV profile of PNTCDA in 1 M $LiNO_3$ solution with a sweep rate of 1 mV s^{-1}. Two pairs of symmetric redox peaks are observed during the oxidation and reduction processes, in the potential ranges of −0.27 to −0.42 V and −0.66 to −0.73 V [versus saturated calomel electrode (SCE)], which can be ascribed to the two continuous steps. In the reduction process, PNTCDA was first transferred to the radical anion (PNTCDA^{--}) and then to the dianion (PNTCDA^{2-}) accompanied by the incorporation of Li^+ ions forming lithium enolate groups (14). In the corresponding oxidation process, Li^+ ions were removed from the lithium enolate groups (C-O-Li), and carbonyl groups (C=O) were rebuilt. The charge/discharge profile with a current density of 1 A g^{-1} is given in Fig. 2B, where the slope plateau from −0.4 to −0.8 V versus SCE should be related to the two-step reduction of the carbonyl groups in the PNTCDA units during the discharge course, whereas the slope plateau in the charge curve corresponds to the reoxidation of the enolate groups. Moreover, a discharge capacitance of 154 mAh g^{-1} also indicates that the two carbonyl groups in PNTCDA are reduced to form Li_2PNTC-DA, which is consistent with the structure proposed in Fig. 1B. The CV profile and charge/discharge profile of PNTCDA in 1 M $NaNO_3$ tested under the same conditions are given in Fig. 2, C and D, respectively. It can be observed that the Na-storage behavior of PNTCDA (Fig. 2, C and D) is the same as its Li-storage behavior, indicating that the reversible charge storage of PNTCDA is not influenced by the type of cation (Li^+ or Na^+). The charge storage of PNTCDA depends on the enolization process, which is different from the intercalation/de-intercalation
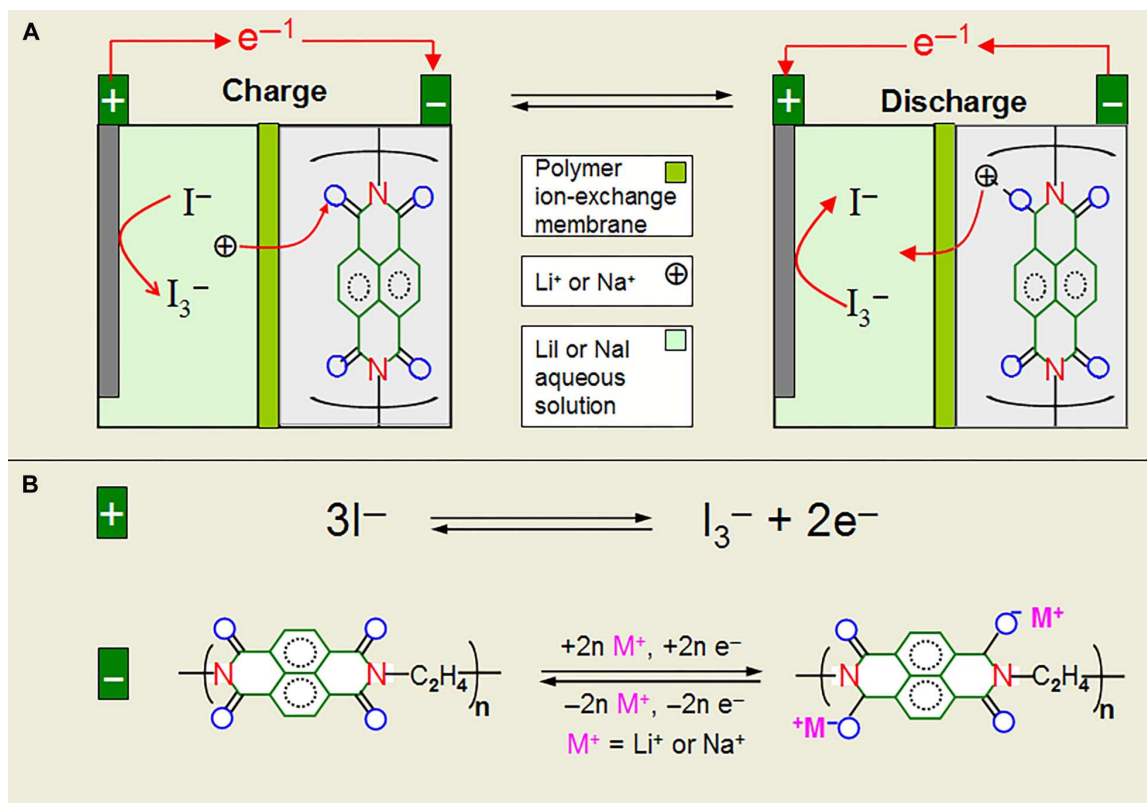

Fig. 1. Schematic illustration of cell structure and electrode reactions. (**A**) Cell structure schematic illustration. (**B**) Electrode reactions.
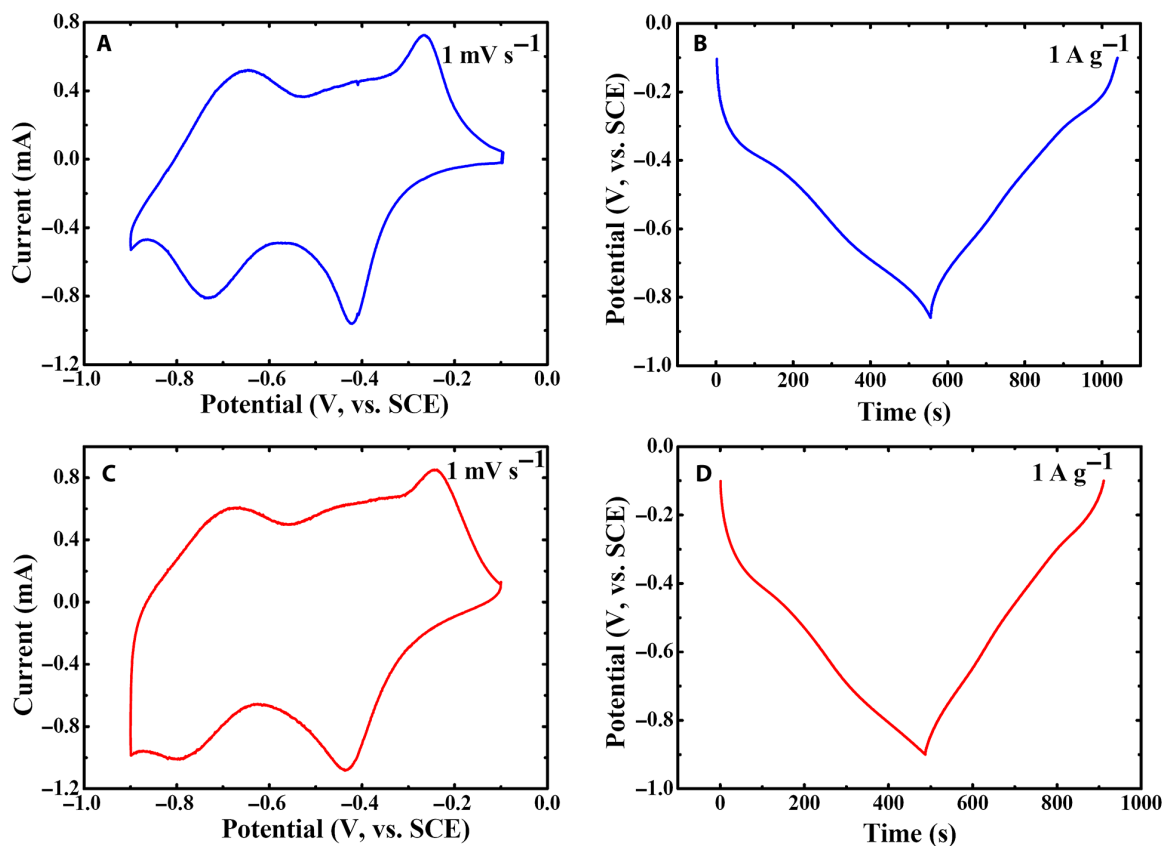
Fig. 2. Electrochemical behavior of the PNTCDA-based electrode in aqueous electrolyte. (**A**) CV test in LiNO$_3$ solution. (**B**) Galvanostatic charge/discharge in LiNO$_3$ solution. (**C**) CV test in NaNO$_3$ solution. (**D**) Galvanostatic charge/discharge in NaNO$_3$ solution.

or dissolution/deposition mechanism of conventional rechargeable batteries. When PNTCDA is combined with cation with +1 charge state (for example, Li or Na) during the reduction process (that is, discharge process), the charge redistribution occurs within the conjugated aromatic molecule (*14*). Charge reverses the discharge process. The special charge storage mechanism in the chemical bonds causes minimum damages and volume expansion of the primary structures (*14, 25–27*), thus ensuring the outstanding structural stability of PNTCDA over discharge/charge cycles. The electrochemical behavior of liquid cathode (that is, I$^-$/I$_3^-$ solution containing Li$^+$ or Na$^+$) was also investigated in a three-electrode system (figs. S2 and S3). The electrochemical behavior of I$^-$/I$_3^-$ redox couple in aqueous electrolyte mainly falls in the potential window of 0 to 0.7 V versus SCE (fig. S3).

Electrode kinetics investigation

CV is an efficient tool to investigate the kinetics of electrode reaction. In theory, the voltammetric response of an electrode-active material at various sweep rates can be summarized as follows (*28–31*)

$$i = av^b \tag{1}$$

in which the measured current (*i*) at a fixed potential obeys a power-law relationship with the potential sweep rate (*v*). For a redox reaction limited by semi-infinite diffusion, the peak current *i* varies with $v^{1/2}$ (that is, *b* = 0.5); for a capacitive process, it varies with *v* (that is, *b* = 1) (*28*). It has been well demonstrated that over a wide range of sweep rates *v*, the

conventional rechargeable battery electrode materials [for example, LiFePO$_4$, LiCoO$_2$, LiMn$_2$O$_4$, graphite, and Ni(OH)$_2$] have a *b* value of ≈0.5, whereas for the pseudocapacitor materials (such as RuO$_x$, MnO$_2$, and Nb$_2$O$_5$), *b* ≈ 1.0. This should be the key reason for the much higher power of supercapacitors, compared with rechargeable batteries (such as Li-ion, Ni-MH, Ni-Cd, and Pb-acid batteries). As shown in Fig. 3, A and B, the redox reaction (that is, charge/discharge process) of the PNTCDA-based electrode in aqueous LiNO$_3$ electrolyte has a *b* value of 0.88, indicating a pseudocapacitive characteristic. Similarly, the PNTCDA-based electrode exhibits the pseudocapacitive characteristic of sodium storage in aqueous NaNO$_3$ electrolyte (Fig. 3, C and D). The results in Fig. 3 demonstrate that the electrode kinetics of PNTCDA is not limited by the diffusion process. That is, its charge storage behavior exhibits a pseudocapacitive characteristic. In addition, CV investigation at different sweep rates was also carried out to study the electrode kinetics of the I$^-$/I$_3^-$-based aqueous electrode. As shown in Fig. 4, the redox of I$^-$/I$_3^-$ has a *b* value of 0.75 in Li$^+$-based aqueous electrolyte and a *b* value of 0.78 in Na$^+$-based aqueous electrolyte, respectively. This result indicates that the I$^-$/I$_3^-$ redox reaction accompanied by Li$^+$/Na$^+$ exchange through the Nafion film still is not controlled by semi-infinite diffusion. However, in previous Li-I$_2$ batteries (*10*), the electrode kinetics of the I$^-$/I$_3^-$ liquid electrode is limited by the Li$^+$ diffusion across the Li ion conductive Li$_2$O-Al$_2$O$_3$-TiO$_2$-P$_2$O$_5$ glass ceramic that was used to separate the I$^-$/I$_3^-$ liquid electrode and Li anode. Here, the I$^-$/I$_3^-$ liquid cathode and the PNTCDA anode (or I$^-$/I$_3^-$ liquid electrode and counter/reference electrode in the three-electrode investigation) are separated by conventional Nafion film, which displays much higher
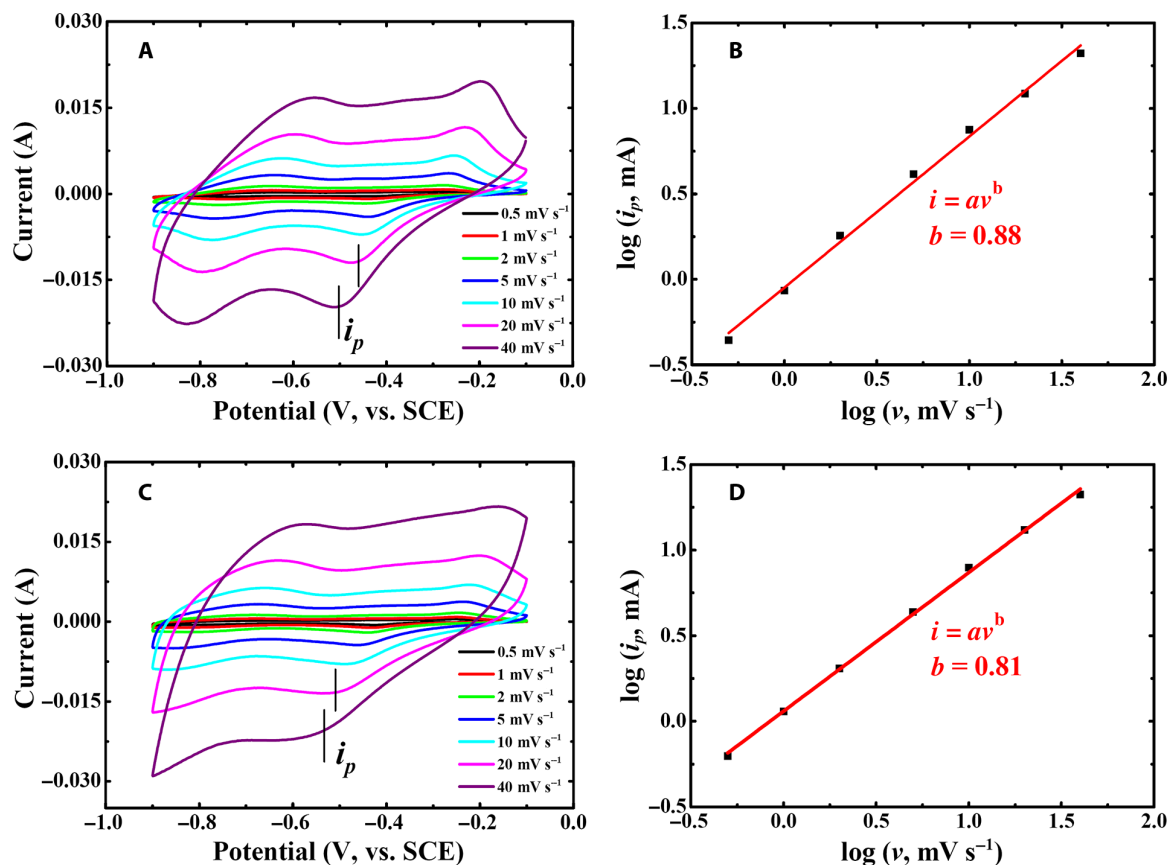
Fig. 3. CV curves at different sweep rates (v) and corresponding log i_p versus log v of the PNTCDA composite electrode in 1 M LiNO$_3$ or NaNO$_3$. (**A** and **B**) LiNO$_3$ solution (1 M). (**C** and **D**) NaNO$_3$ solution (1 M).

conductivity than the ceramic separator. As shown in Figs. 3 and 4, the b value (0.75 or 0.78) for the I^-/I_3^- redox couple in Li$^+$ (or Na$^+$)–based aqueous electrolyte is lower than that (0.88 or 0.81) for the PNTCDA-based electrode. In theory, the redox process of the I^-/I_3^- couple in aqueous electrolyte solution should be very fast. The lower b value may be due to the ion-exchange membrane (that is, Nafion film) slightly slowing down the ion diffusion in the liquid electrode.

Electrochemical performance of a full cell

After the electrochemical investigation for single electrodes, PNTCDA and the aqueous solution containing I^-/I_3^- and Li$^+$ (or Na$^+$) are used as anode and cathode, respectively, to form an aqueous Li (or Na)-ion battery (fig. S4). Figure 5 shows the electrochemical performance of the aqueous Li-ion battery that is based on PNTCDA anode and liquid cathode. As shown in Fig. 5A, the full cell can be cycled within the voltage window of 0 to 1.6 V, which is consistent with the potential difference between the cathode and the anode observed earlier. The specific capacity (mAh g^{-1}) and the current density (A g^{-1}) are calculated on the basis of the mass of anode material. A rate of nC corresponds to a full charge/discharge in 1/nh (according to the theoretical capacity of 183 mAh g^{-1} of PNTCDA, the rate of 1C indicates a discharge/charge current density of 183 mA g^{-1}). It can be observed that the full cell delivers a discharge capacity of 157 mAh g^{-1} at a current density of 1 A g^{-1}, which is equal to 5.5C in terms of C-rate discharge. At a current density of 20 A g^{-1} (110C; 33 s to total charge or discharge), more than 90 mAh g^{-1} can

still be achieved, and a capacity of 56 mAh g^{-1} is obtained at 40 A g^{-1} (220C; 16.5 s to full charge or discharge). Even at a much higher current density of 100 A g^{-1} (550C; indicating 6.6 s to full charge or discharge), the cell can still deliver a capacity of 25 mAh g^{-1}. The extremely high rates are much higher than that of current rechargeable batteries and even close to that of supercapacitors. Such an extremely high-rate performance suggests that the reaction kinetics of both anode (PNTCDA) and liquid cathode (I^-/I_3^- solution) are not limited by the ion diffusion and/or phase conversion process, which is consistent with the three-electrode investigation (Figs. 3 and 4). As presented in Fig. 5B, the cell exhibits a stable cycling performance at a current density of 10 A g^{-1} and keeps its columbic efficiency around 100% during successive 50,000 cycles. The high columbic efficiency achieved indicates that the crossover of I^- or I_3^- is negligible, which is consistent with a recent report on Zn-polyiodide flow battery using Nafion membrane (*3*). The stability is further demonstrated by the enlargement of cycle performance over 0 to 5000 cycles, as shown in Fig. 5B. Such an excellent cyclability can be attributed to both the electrochemical reversibility and the structural stability of the electrode materials, including the PNTCDA anode and the I^-/I_3^- redox couple–based aqueous cathode. Our recent investigation indicates that the PNTCDA-based anode can be used as an O$_2$ self-elimination electrode (*32*), which potentially alleviates the O$_2$-induced capacity fading in aqueous batteries that is demonstrated in our previous report (*16*). However, there is still capacity fading to some extent. As can be seen in Fig. 5B, the capacity retention is about
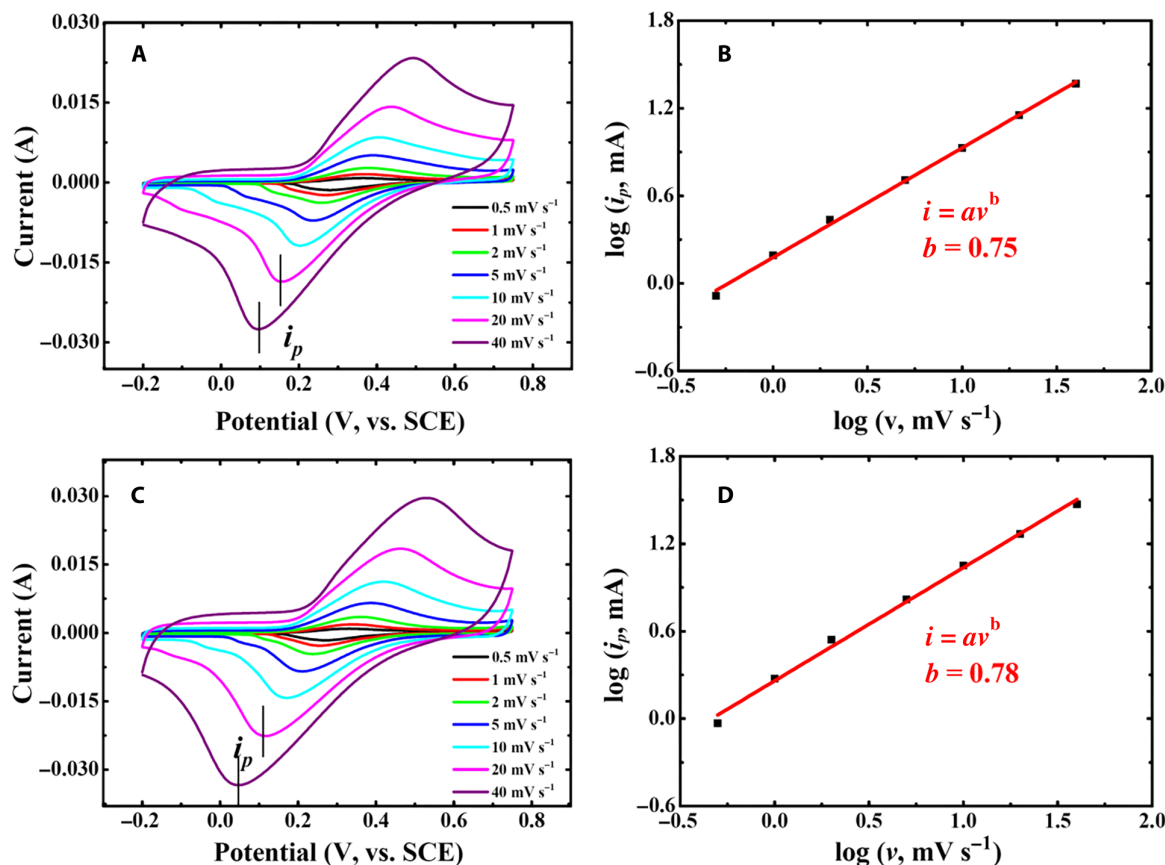
Fig. 4. CV curves at different sweep rates (*v*) and corresponding log *i*$_p$ versus log *v* of the I$^-$/I$_3^-$-based liquid electrode. (A and B) LiI (0.1 M) + I$_2$ (0.01 M) + LiNO$_3$ (1 M) solution. **(C and D)** NaI (0.1 M) + I$_2$ (0.01 M) + NaNO$_3$ (1 M) solution. The experimental conditions are the same as those described in fig. S3, and the experiment was also conducted through the special three-electrode cell shown in fig. S2.

70% over 50,000 cycles. This can be ascribed to the water evaporation and the consequent resistance increase during the long-time charge/discharge process. In addition, current collector passivation may also result in the increase of resistance. This issue will be further investigated in our future technological study.

Because the capacity performance of the PNTCDA anode and the I$^-$/I$_3^-$ redox couple–based liquid cathode does not depend on the cation type (Li$^+$ or Na$^+$), the electrochemical performance of the full cell using electrolyte containing Na$^+$ is expected to be similar to that of the full cell using electrolyte containing Li$^+$. To clarify this point, aqueous Na-ion battery based on PNTCDA anode and liquid cathode was fabricated and investigated under the same conditions. When cycled in the voltage window of 0 to 1.6 V at a current density of 1 A g^{-1} (or the rate of 5.5C), the aqueous Na-ion battery shows a discharge capacity of 140 mAh g^{-1} (Fig. 6A), which is close to that of Li-ion battery tested under the same conditions. The rate capability of aqueous Na-ion battery was also tested, and it delivers a high capacity of 95 mAh g^{-1} at a high current density of 20 A g^{-1} (110C; 33 s to total charge or discharge). When a much higher current density of 40 A g^{-1} (rate of 220C; 16.5 s to full charge or discharge) was applied, the discharge capacity can still reach 59 mAh g^{-1} with a high columbic efficiency of about 100%. Even at an extremely high current density of 100 A g^{-1} (550C; indicating 6.6 s to full charge or discharge), the Na ion–based cell can still deliver a capacity of 28 mAh g^{-1}, which is almost the same as that of the aqueous Li-ion

battery mentioned earlier. As shown in Fig. 6B, the cell can be stably cycled over 50,000 times with a capacity retention of 70%, which is close to that of the aqueous Li-ion battery mentioned earlier. It should be noted that the high-rate performance shown in Fig. 5A or 6A was achieved by using the low-concentration aqueous cathode (0.1 M LiI or NaI) and the PNTCDA anode with low mass loading of active material (~1 mg cm^{-2}), which is used to confirm the fast kinetics of electrodes. In practical applications, high-concentration aqueous cathode and PNTCDA anode with high mass loading of active material are quite necessary. Therefore, we used the higher-concentration aqueous cathode (5 M LiI or NaI) and the PNTCDA anode with higher mass loading of active material (5 mg cm^{-2}) to construct a full cell, and investigated its rate performance by galvanostatic charge/discharge measurements (fig. S5). The results indicate that the viscosity of aqueous cathode and the resistance of PNTCDA anode can limit the rate performance to some extent. This issue should be further investigated in future studies.

DISCUSSION

To further demonstrate the promising application of such a full battery system, we evaluated the energy density based on the electrode-active materials, and compared it with the values given in recent reports. In view of the average cell voltage, the specific capacities of electrode materials (that is, LiI/NaI and PNTCDA), and the high solubility of

LiI or NaI, the calculated energy densities of the aqueous Li-ion battery and Na-ion battery are ~65.3 and ~63.8 Wh kg^{-1}, respectively (detailed calculations are given in the Supplementary Materials). The energy density (65.3 or 63.8 Wh kg^{-1}) is close to that of current aqueous batteries for stationary or grid-level energy storage, such as the Prussian blue analog aqueous battery (45/27 Wh kg^{-1}) [19, 20], the LiTi$_2$(PO$_4$)$_3$/LiFePO$_4$ aqueous Li-ion battery (~50 Wh kg^{-1}) [16], the NaTi$_2$(PO$_4$)$_3$/Na$_{0.44}$MnO$_2$ aqueous Li-ion battery (~33 Wh kg^{-1}) [17], and the organic/inorganic aqueous flow battery (50 Wh kg^{-1}) [7]. However, the new aqueous Li (or Na)-ion battery displays a super-long cycle life (50,000 cycles), which is much higher than that of any other rechargeable batteries. Furthermore, it is demonstrated that its electrode reactions are not totally limited by the ion diffusion process, whereas the kinetics of electrode reactions in conventional Li (or Na)-ion batteries is generally limited by the Li$^+$ (or Na$^+$) diffusion within the crystalline framework of electrode materials. As a result, the new Li (or Na)-ion battery can be cycled at a high rate of 550C (100 A g^{-1}; 6.6 s to full charge or discharge), indicating a supercapacitor-like high power. It is more important that there are no metal element–based redox reactions in this new battery system, where the Li$^+$ (or Na$^+$) is only used for charge transfer. In addition, because of the liquid characteristic of cathode, the cell can be operated as a single-flow battery in practical applications. Finally, the new-type Li (or Na)-ion battery is an environment-friendly system because the iodide-based cathode, the polyimide-based anode, and the neutral (pH ~ 7) aqueous electrolyte all have low toxicity. It should be noted that most current batteries involve toxic and/or environmentally unfriendly factors, such as toxic nonaqueous electrolyte in current Li-ion batteries, acid/alkaline electrolyte in Ni-MH/lead-acid batteries, and toxic electrode materials (for example, Pb in lead-acid batteries, Cd in Ni-Cd batteries, VO$_x$ in vanadium flow batteries, and Br$_2$ in Zn-Br$_2$ flow batteries).

In summary, a new-type aqueous Li (or Na)-ion battery has been proposed by using a polymer Li$^+$ (or Na$^+$) exchange membrane to separate a solid-state polymer anode and a liquid cathode containing water-soluble inorganic redox couples. Such a system can exhibit a supercapacitor-like high-rate performance and a super-long cycle life because the kinetics of both electrode reactions are limited neither by the ion diffusion process nor by phase conversion. This finding not only provides a promising solution for grid-scale energy storage but also brings a new idea for battery design.
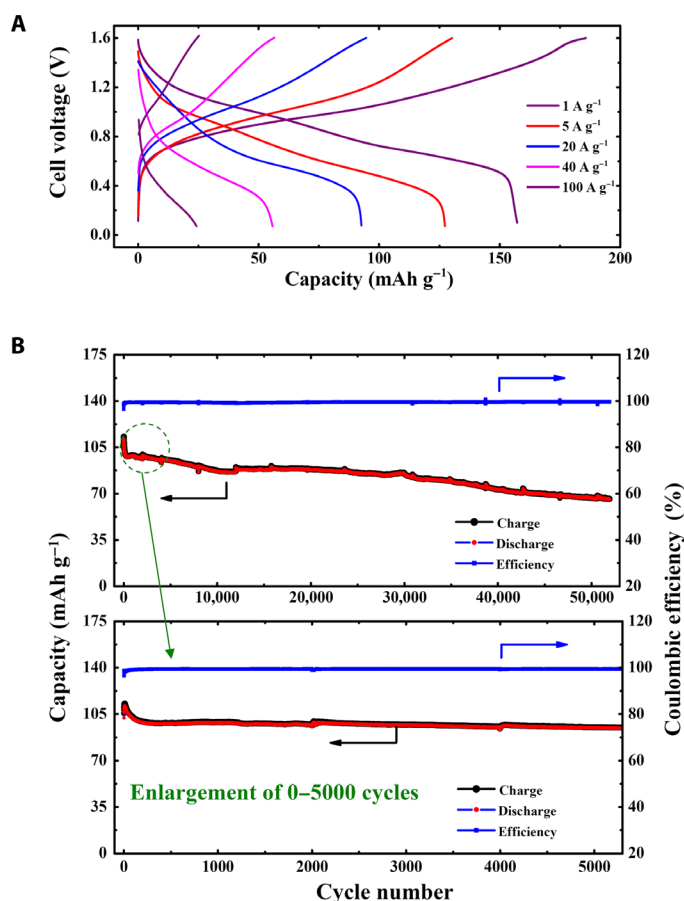

Fig. 5. Electrochemical performance of aqueous Li-ion battery based on solid PNTCDA anode and liquid I$^-$/I$_3^-$ cathode. (**A**) Galvanostatic charge/discharge at different current densities. (**B**) Cycle life. [Current density (A g^{-1}) and specific capacity (mAh g^{-1}) are calculated on the basis of the anode material.]
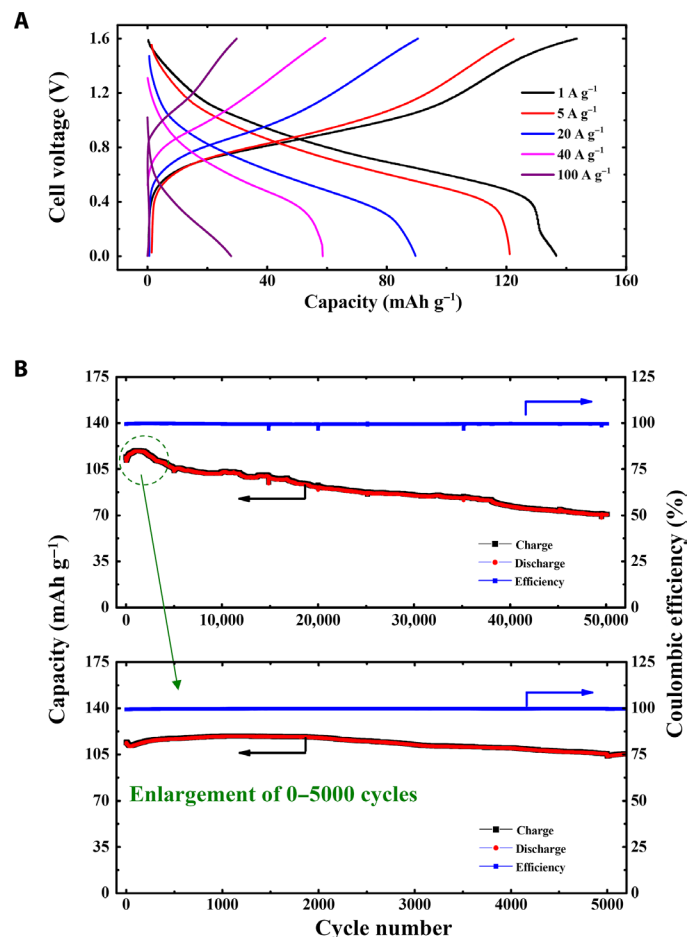

Fig. 6. Electrochemical performance of aqueous Na-ion battery based on solid PNTCDA anode and liquid I$^-$/I$_3^-$ cathode. (**A**) Galvanostatic charge/discharge at different current densities. (**B**) Cycle life. [Current density (A g^{-1}) and specific capacity (mAh g^{-1}) are calculated on the basis of the anode material.]

MATERIALS AND METHODS

Synthesis of electrode materials

The NTCDA-derived polyimide (that is, PNTCDA) was synthesized from NTCDA and ethylene diamine (EDA) according to a previous report (24). In a typical synthesis, equimolar commercialized NTCDA and EDA were added in the solvent N-methylpyrrolidone (NMP) and reacted under reflux for 6 hours. The obtained product was filtrated, washed several times with ethanol and NMP, dried at 120°C in air for 12 hours, and then heated in nitrogen atmosphere for 8 hours at 300°C. The reagents (for example, NTCDA, EDA, LiI, and NaI) were purchased from Sinopharm Chemical Reagent Co. Ltd.

Electrode preparation and battery assembly

The polymer-based anode was obtained by mixing 60 wt % active material, 30 wt % Ketjen Black (KB) as conductive agent, and 10 wt % polytetrafluoroethylene (PTFE) as binder. For a typical preparation, PNTCDA, KB, and PTFE were dissolved in isopropanol to form a slurry with the weight ratio mentioned above, and then the slurry was rolled into a film electrode. An aqueous solution containing 0.1 M LiI (or NaI), 0.01 M I_2, and 1 M $LiNO_3$ (or $NaNO_3$) was used as the liquid cathode, and a carbon (that is, KB)–loaded stainless steel mesh was used as the current collector for the liquid cathode. The KB carbon powder and PTFE were mixed at an 80:20 mass ratio in isopropanol to form a slurry, which was then rolled into a film. Next, the carbon-loaded current collector was obtained by pressing the KB-based film on a stainless steel mesh with a KB loading of 1 mg cm^{-2}. For full cell assembly, 200 μl of the aqueous cathode and the $LiNO_3$ (or $NaNO_3$) solution–wetted anode was separated with Nafion 117, as shown in Fig. 1A (or see fig. S4 for detailed information). The mass loading of PNTCDA in the anode was ~1 mg cm^{-2}. Before cell assembly, the commercial Nafion 117 film was alternately immersed in 1 M $LiNO_3$ (or $NaNO_3$) solution and washed with 1 M $LiNO_3$ (or $NaNO_3$) solution until the pH value reached ~7. The pH value of electrolyte solution in the full cell was ~7.

Electrochemical measurements

Electrochemical tests including rate performance and cycle performance for the full cell were performed on the HOKUTO DENKO Battery Charge/Discharge System HJ Series controlled by a computer. CV and galvanostatic charge/discharge measurements of the PNTCDA electrode in 1 M $LiNO_3$ solution (or 1 M $NaNO_3$ solution) were investigated on an electrochemistry workstation (CHI 660) with a three-electrode system, where an SCE and active carbon were used as reference and counter electrodes, respectively. The same three-electrode measurements were also conducted for the aqueous cathode, where the aqueous electrode and the reference/counter electrode were separated by Nafion film, as shown in fig. S2.

SUPPLEMENTARY MATERIALS

Supplementary material for this article is available at http://advances.sciencemag.org/cgi/content/full/2/1/e1501038/DC1
Fig. S1. FT-IR spectrum of as-prepared PNTCDA.
Fig. S2. Schematic illustration of the cell for aqueous electrode investigation with a three-electrode system.
Fig. S3. Electrochemical behavior of the I⁻/I₃⁻–based liquid electrode.
Fig. S4. Schematically showing the assembly of a full cell.
Fig. S5. Rate performance of a full cell using a high-concentration aqueous cathode (5 M LiI or NaI).
Calculation of energy density
References (33–35)

REFERENCES AND NOTES

1. G. L. Soloveichik, Electrochemistry: Metal-free energy storage. *Nature* **505**, 163–165 (2014).
2. B. Dunn, H. Kamath, J.-M. Tarascon, Electrical energy storage for the grid: A battery of choices. *Science* **334**, 928–935 (2011).
3. B. Li, Z. Nie, M. Vijayakumar, G. Li, J. Liu, V. Sprenkle, W. Wang, Ambipolar zinc-polyiodide electrolyte for a high-energy density aqueous redox flow battery. *Nat. Commun.* **6**, 6303 (2015).
4. Z. Yang, J. Zhang, M. C. W. Kintner-Meyer, X. Lu, D. Choi, J. P. Lemmon, J. Liu, Electrochemical energy storage for green grid. *Chem. Rev.* **111**, 3577–3613 (2011).
5. C. Chen, Y. Wen, X. Hu, X. Ji, M. Yan, L. Mai, P. Hu, B. Shan, Y. Huang, Na⁺ intercalation pseudo-capacitance in graphene-coupled titanium oxide enabling ultra-fast sodium storage and long-term cycling. *Nat. Commun.* **6**, 6929 (2015).
6. K. Wang, K. Jiang, B. Chung, T. Ouchi, P. J. Burke, D. A. Boysen, D. J. Bradwell, H. Kim, U. Muecke, D. R. Sadoway, Lithium–antimony–lead liquid metal battery for grid-level energy storage. *Nature* **514**, 348–350 (2014).
7. B. Huskinson, M. P. Marshak, C. Suh, S. Er, M. R. Gerhardt, C. J. Galvin, X. Chen, A. Aspuru-Guzik, R. G. Gordon, M. J. Aziz, A metal-free organic–inorganic aqueous flow battery. *Nature* **505**, 195–198 (2014).
8. M. Winter, R. J. Brodd, What are batteries, fuel cells, and supercapacitors? *Chem. Rev.* **104**, 4245–4270 (2004).
9. M. Armand, J.-M. Tarascon, Building better batteries. *Nature* **451**, 652–657 (2008).
10. Y. Zhao, L. Wang, H. R. Byon, High-performance rechargeable lithium–iodine batteries using triiodide/iodide redox couples in an aqueous cathode. *Nat. Commun.* **4**, 1896 (2013).
11. Y. Zhao, N. B. Mercier, H. R. Byon, An aqueous lithium–iodine battery with solid polymer electrolyte-coated metallic lithium anode. *ChemPlusChem* **80**, 344–348 (2015).
12. Y. Zhao, M. Hong, N. Bonnet Mercier, G. Yu, H. C. Choi, H. R. Byon, A 3.5 V lithium–iodine hybrid redox battery with vertically aligned carbon nanotube current collector. *Nano Lett.* **14**, 1085–1092 (2014).
13. Y. Zhao, H. R. Byon, High-performance lithium-iodine flow battery. *Adv. Energy Mater.* **3**, 1630–1635 (2013).
14. H. Kim, J. Hong, K.-Y. Park, H. Kim, S.-W. Kim, K. Kang, Aqueous rechargeable Li and Na ion batteries. *Chem. Rev.* **114**, 11788–11827 (2014).
15. Y. Wang, J. Yi, Y. Xia, Recent progress in aqueous lithium-ion batteries. *Adv. Energy Mater.* **2**, 830–840 (2012).
16. J.-Y. Luo, W.-J. Cui, P. He, Y.-Y. Xia, Raising the cycling stability of aqueous lithium-ion batteries by eliminating oxygen in the electrolyte. *Nat. Chem.* **2**, 760–765 (2010).
17. Z. Li, D. Young, K. Xiang, W. C. Carter, Y.-M. Chiang, Towards high power high energy aqueous sodium-ion batteries: The NaTi₂(PO₄)₃/Na₀.₄₄MnO₂ system. *Adv. Energy Mater.* **3**, 290–294 (2013).
18. Y. Wang, J. Liu, B. Lee, R. Qiao, Z. Yang, S. Xu, X. Yu, L. Gu, Y.-S. Hu, W. Yang, K. Kang, H. Li, X.-Q. Yang, L. Chen, X. Huang, Ti-substituted tunnel-type Na₀.₄₄MnO₂ oxide as a negative electrode for aqueous sodium-ion batteries. *Nat. Commun.* **6**, 6401 (2015).
19. M. Pasta, C. D. Wessells, R. A. Huggins, Y. Cui, A high-rate and long cycle life aqueous electrolyte battery for grid-scale energy storage. *Nat. Commun.* **3**, 1149 (2012).
20. M. Pasta, C. D. Wessells, N. Liu, J. Nelson, M. T. McDowell, R. A. Huggins, M. F. Toney, Y. Cui, Full open-framework batteries for stationary energy storage. *Nat. Commun.* **5**, 3007 (2014).
21. X.-Y. Wu, M.-Y. Sun, Y.-F. Shen, J.-F. Qian, Y.-L. Cao, X.-P. Ai, H.-X. Yang, Energetic aqueous rechargeable sodium-ion battery based on Na₂CuFe(CN)₆–NaTi₂(PO₄)₃ intercalation chemistry. *ChemSusChem* **7**, 407–411 (2014).
22. G. Wang, L. Fu, N. Zhao, L. Yang, Y. Wu, H. Wu, An aqueous rechargeable lithium battery with good cycling performance. *Angew. Chem. Int. Ed.* **46**, 295–297 (2007).
23. H. Qin, Z. P. Song, H. Zhan, Y. H. Zhou, Aqueous rechargeable alkali-ion batteries with polyimide anode. *J. Power Sources* **249**, 367–372 (2014).
24. L. Chen, W. Li, Y. Wang, C. Wang, Y. Xia, Polyimide as anode electrode material for rechargeable sodium batteries. *RSC Adv.* **4**, 25369–25373 (2014).
25. G. S. Vadehra, R. P. Maloney, M. A. Garcia-Garibay, B. Dunn, Naphthalene diimide based materials with adjustable redox potentials: Evaluation for organic lithium-ion batteries. *Chem. Mater.* **26**, 7151–7157 (2014).
26. W. Luo, M. Allen, V. Raju, X. Ji, An organic pigment as a high-performance cathode for sodium-ion batteries. *Adv. Energy Mater.* **4**, 1400554 (2014).
27. Z. Song, H. Zhan, Y. Zhou, Polyimides: Promising energy-storage materials. *Angew. Chem. Int. Ed.* **49**, 8444–8448 (2010).
28. P. Simon, Y. Gogotsi, B. Dunn, Where do batteries end and supercapacitors begin? *Science* **343**, 1210–1211 (2014).
29. T. Brezesinski, J. Wang, S. H. Tolbert, B. Dunn, Ordered mesoporous α-MoO₃ with iso-oriented nanocrystalline walls for thin-film pseudocapacitors. *Nat. Mater.* **9**, 146–151 (2010).

30. V. Augustyn, J. Come, M. A. Lowe, J. W. Kim, P.-L. Taberna, S. H. Tolbert, H. D. Abruña, P. Simon, B. Dunn, High-rate electrochemical energy storage through Li^+ intercalation pseudocapacitance. *Nat. Mater.* **12**, 518–522 (2013).

31. Y. Wang, Z. Hong, M. Wei, Y. Xia, Layered $H_2Ti_6O_{13}$-nanowires: A new promising pseudocapacitive material in non-aqueous electrolyte. *Adv. Funct. Mater.* **22**, 5185–5193 (2012).

32. L. Chen, W. Li, Z. Guo, Y. Wang, C. Wang, Y. Che, Y. Xia, Aqueous lithium-ion batteries using O_2 self-elimination polyimides electrodes. *J. Electrochem. Soc.* **162**, A1972–A1977 (2015).

33. H.-g. Wang, S. Yuan, D.-l. Ma, X.-l. Huang, F.-l. Meng, X.-b. Zhang, Tailored aromatic carbonyl derivative polyimides for high-power and long-cycle sodium-organic batteries. *Adv. Energy Mater.* **4**, 1301651 (2014).

34. D. J. Kim, Y. H. Jung, K. K. Bharathi, S. H. Je, D. K. Kim, A. Coskun, J. W. Choi, An aqueous sodium ion hybrid battery incorporating an organic compound and a Prussian blue derivative. *Adv. Energy Mater.* **4**, 1400133 (2014).

35. H. Wu, S. A. Shevlin, Q. Meng, W. Guo, Y. Meng, K. Lu, Z. Wei, Z. Guo, Flexible and binder-free organic cathode for high-performance lithium-ion batteries. *Adv. Mater.* **26**, 3338–3343 (2014).

Citation: X. Dong, L. Chen, J. Liu, S. Haller, Y. Wang, Y. Xia, Environmentally-friendly aqueous Li (or Na)-ion battery with fast electrode kinetics and super-long life. *Sci. Adv.* **2**, e1501038 (2016).